The Journal of Veterinary Medical Science

NOTE

Anatomy

Morphometric analysis of cornea in the *Slc39a13*/*Zip13*-knockout mice

Takuya HIROSE[1)], Ippei SUZUKI[1)], Naoki TAKAHASHI[1)], Toshiyuki FUKADA[2)], Prasarn TANGKAWATTANA[1,3)]* and Kazushige TAKEHANA[1)]

[1)]Laboratory of Microanatomy, School of Veterinary Medicine, Rakuno Gakuen University, Ebetsu, Hokkaido 069-8501, Japan
[2)]Molecular and Cellular Physiology, Faculty of Pharmaceutical Sciences, Tokushima Bunri University, Tokushima 770-8055, Japan
[3)]Department of Veterinary Anatomy, Faculty of Veterinary Medicine, Khon Kaen University, Khon Kaen 40002, Thailand

J. Vet. Med. Sci.
80(5): 814–818, 2018
doi: 10.1292/jvms.18-0019

Received: 11 January 2018
Accepted: 12 March 2018
Published online in J-STAGE: 22 March 2018

ABSTRACT. Ehlers-Danlos syndrome (EDS) is a group of hereditary diseases caused by mutation of extracellular matrix-related genes. Recently, spondylodysplastic EDS-*Zip13* (spEDS-*Zip13*: OMIM 612350) was recognized as a new EDS type. This current study could reveal various morphometric differences of collagenous population in the proper substance of cornea between the wild type and spEDS-*Zip13*-knockout (*Zip13*-KO) mice. Blockade of Smad-signaling pathway might initiate these alterations. Predilected dissimilarity in level of transcriptional activity probably dictated morphology of keratocyte and shape and electron density of its nucleus. In addition, the imbalance of proteoglycans and glycosaminoglycans would also affect the diameter and arrangement of collagen fibrils. These findings would be considered as vulnerable characteristics of corneal stroma of the *Zip13*-KO mice.

KEY WORDS: collagen fibril, cornea, morphometry, *Slc39a13*/*Zip13*-knockout mice

Ehlers-Danlos syndrome (EDS) is a group of hereditary diseases caused by mutation of extracellular matrix (ECM)-related genes, such as COL1A1, COL3A1 and COL5A1 [6]. Major phenotypes of this syndrome include hyperextension of the skin, hypermobility of joints and fragility of blood vessels [4, 6]. Thus, EDS has been categorized into thirteen subtypes according to its different causes and symptoms [13]. SLC39A13/ZIP13 is a member of the SLC39/ZIP zinc transporter family localizing mainly in the Golgi apparatus of osteoblasts, chondrocytes, odontoblasts and fibroblasts [5]. This protein involves in transporting zinc from the Golgi apparatus to the cytoplasm and controls the nuclear shift of SMAD proteins in TGF-β1 and bone morphogenetic protein (BMP) signaling pathways [2, 3, 7, 16]. After the finding of mutation in SLC39A13/ZIP13 (ZIP13) of three gene types—i.e., *B4GALT7*, *B3GALT6* and *ZIP13*, spondylodysplastic EDS-*ZIP13* (spEDS-*ZIP13*: OMIM 612350) was recognized as a new EDS type [5, 8, 13]. Its clinical expressions were classified into major criteria (including short stature, muscle hypotonia, and bowing of limbs) and minor criteria (including skin hyperextensibility, pes planus, delayed motor development, osteopenia, and delayed cognitive development). Besides, protuberant eyes with bluish sclerae were also included in the minor criteria [13]. spEDS-*ZIP13* as a cause of thin cornea was also reported in 5-week-old *Zip13*-KO mice [7]. The cornea generally consists of five layers—i.e., anterior epithelium, anterior limiting membrane (Bowman's membrane, usually absent in non-primates), proper substance (substantia propria, corneal stroma), posterior limiting membrane (Descemet's membrane), and posterior endothelium. The proper substance with abundant collagen fibers and keratocytes occupies about 90% of the whole corneal thickness [1]. These collagen fibers configure into lamellae and each consecutive lamella usually arranged at almost right angle to each other [11]. Since EDS directly affects integrity of the ECM and eye problems were found in many cases of EDS subtypes and spEDS-*ZIP13* [13], the ECM-rich cornea should be an affected organ of this syndrome. Therefore, this current study performed morphometric analysis of cornea in the wild type (WT) and spEDS-*ZIP13* mice model.

The animal experiments were approved by the Committee on the Ethics of Animal Experiments of Rakuno Gakuen University (#VH15A6, June 15, 2015). Six C57BL/6; 129-SLC39A13^{tm1thir} mice (RBRCR06217), being three *Zip13*-KO and three WT mice, were provided by RIKEN BRC via the National Bio-Resource Project of the MEXT, Japan. Mice of both groups were weaned at the age of 4 weeks. The 12-week-old mice were anesthetized by an intraperitoneal administration of 65 mg/kg pentobarbital (Somnopentyl®, Kyoritsu Pharmaceutical, Tokyo, Japan) and immediately euthanized by exsanguination. Then, the whole eyeball from each mouse was collected. The right fresh eyeball was embedded in OTC compound (Sakura Finetek Japan Co., Ltd., Tokyo,

*Correspondence to: Tangkawattana, P.: prasarn@kku.ac.th

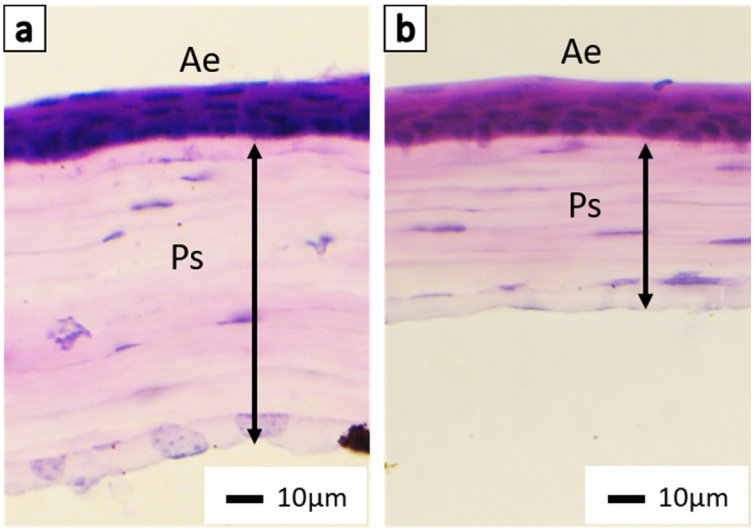

Fig. 1. Light microscopic observation of the central cornea of the WT (a) and *Zip13*-KO mice group (b) with H&E staining. Thickness and appearance of the anterior epithelium (Ae) of both groups had no difference. Nevertheless, proper substance (Ps) in the *Zip13*-KO group was apparently thinner than that of the WT group. [Bars=10 μm].

Table 1. Morphometric analysis of collagen fibrils in cornea of the WT and *Zip13*-KO mice group

Analysis (mean ± standard error)	WT group	*Zip13*-KO group
Thickness of proper substances (μm)	89.1 ± 1.0	41.1 ± 2.7[a)]
Number of collagenous layers	69.3 ± 0.9	68.7 ± 1.2
Thickness of collagenous layers (μm)	1.3 ± 0.01	0.6 ± 0.01[a)]
Diameter of collagen fibrils (nm)	27.4 ± 0.2	22.2 ± 0.9[a)]
Collagen fibril index (%)	34.0 ± 2.5	19.7 ± 2.0[a)]

a) Significantly different in mean ± standard error between groups at $P<0.05$.

Japan). 10-μm-thick sections being cut by cryostat (CM3050S, Leica) were stained with H&E. Three sections of each sample were used in investigating proper substance at the center of cornea and keratocytes in the center and limbus of cornea. The left eyeball was pre-fixed in 3.0% glutaraldehyde in 0.1 M phosphate buffer (pH 7.4) for 2 hr at room temperature and immediately post-fixed in 1.0% osmium tetroxide in 0.1 M phosphate buffer for 1 hr at room temperature. After washed with distilled water, the samples were dehydrated in a graded ethanol series and embedded in Quetol 812 (Nissin EM, Tokyo, Japan). The 60-nm-thick-sections were cut with a Reichert Supernova system (Leica, Vienna, Austria) equipped with a diamond knife, and mounted on a copper grid. Consecutive staining with 0.2% tannic acid + 10% ethanol in water for 15 min, 1.0% uranyl acetate for 5 min, and 1.0% lead citrate for 10 sec was performed. The samples were Investigated with a transmission electron microscopy (TEM) (JEM-1220; JEOL, Tokyo, Japan) at an accelerating voltage of 80 kV. Regards, diameters of 500 collagen fibrils randomly selected from each sample were measured. Collagen Fibril Index (CFI, ratio between collagen's square surface and the sum of collagen and non-collagen's square surfaces) in the ECM was analyzed by Image J software (version 1.48v; National Institutes of Health, Bethesda, MD, U.S.A.). Additionally, the number and thickness of collagenous layer were measured at 5 areas in each sample. Students'*t*-test was applied to compare mean ± standard errors of thickness of corneal epithelium and stroma, thickness and number of collagenous layers, and CFI. Welch's *t*-test was applied for diameter of collagen fibrils. Significant difference was accepted at $P<0.05$.

Apparently, there was no difference in thickness and histological appearance of the anterior epithelium between both groups. Nevertheless, thickness of the proper substance of the WT group (89.1 ± 9.1 μm) was approximately twice to that of the *Zip13*-KO group (41.1 ± 3.0 μm) with significant difference at $P=0.018$ (Fig. 1, Table 1). Although number of collagenous layers between the two groups (69.3 ± 0.9 layers in the WT group and 68.7 ± 1.2 layers in the *Zip13*-KO group) was not different ($P=0.67$), thickness of collagenous layer (1.3 ± 0.01 μm in the WT group and 0.6 ± 0.01 μm in the *Zip13*-KO group) was significantly different at $P<0.001$ (Fig. 2, Table 1). The diameter of collagen fibrils between the WT group (27.4 ± 0.2 nm) and the *Zip13*-KO group (22.2 ± 0.9 nm) was significantly different at $P=0.030$ (Fig. 2, Table 1). In addition, CFI of the *Zip13*-KO group (19.7 ± 2.0%) was significantly decreased upon comparing with that of the WT group (34.0 ± 2.5%) at $P=0.011$ (Fig. 2, Table 1). Each collagen fibril in the collagenous layer of the WT mice arranged parallel to each other while that of the *Zip13*-KO mice was in a random fashion (Fig. 2).

Morphology of keratocytes in both groups was found to have positional predilection (Fig. 3). Keratocytes in the central cornea of the WT mice and limbus of both groups appeared to have both elongated and bullet shape. But major keratocytic population in the central cornea of the *Zip13*-KO mice had elongated shape. Electron density in nucleus of the elongated keratocytes was lower than that of the bullet-shaped keratocytes (Fig. 4).

Although ocular symptoms and thin cornea in the spEDS patients and *Zip13*-KO mice were reported in previous studies [7, 14], subcorneal pathology pertaining to those cases was still unclear. Nevertheless, this study could reveal major vulnerable characteristics in the proper substance layer of cornea in the *Zip13*-KO mice, including thickness, keratocytic morphology, number of collagenous layer, CFI, and orientation of collagen fibrils. CFI value is affected by collagen fibril diameter and distance between collagen fibrils. The decrease of collagen fibril diameter about 20% can decrease CFI about 36%. Reversely, the decrease of CFI about 42% in this investigation would be the result of the spreading of collagen fibril distance. Such spreading would then be

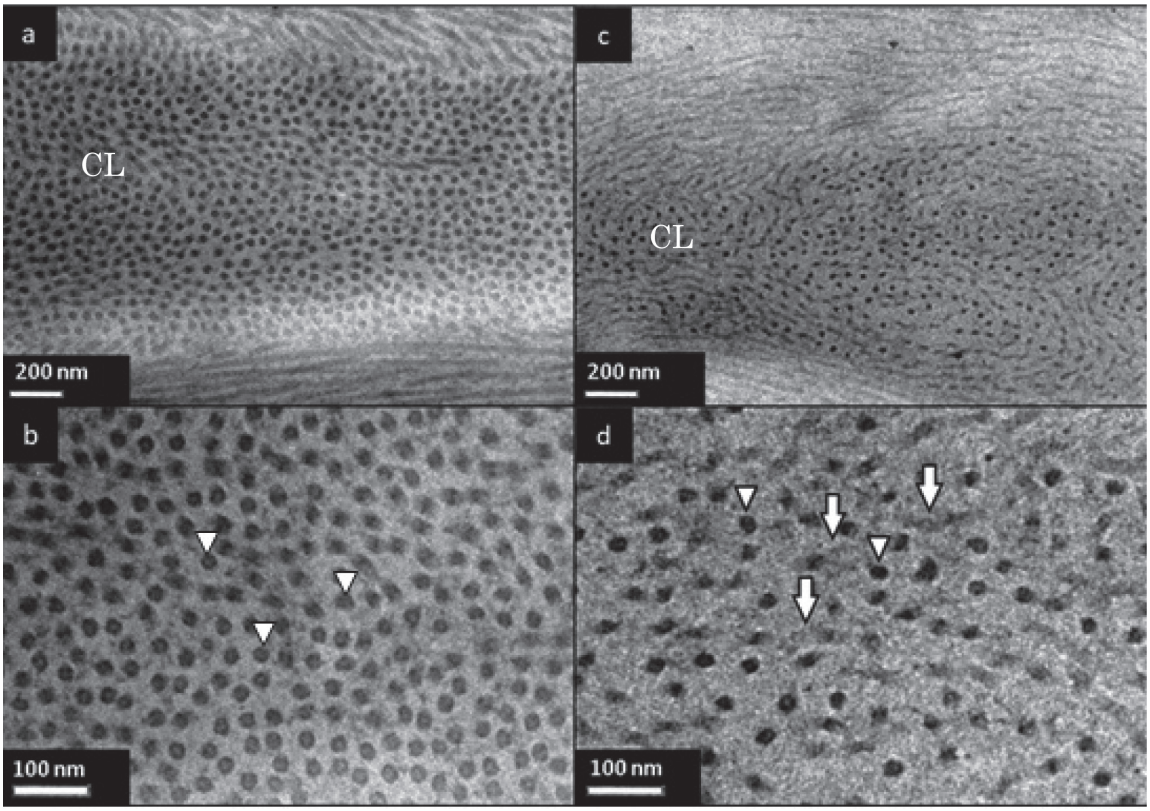

Fig. 2. TEM observation of collagen fibrils in the collagenous layer (CL) of the central cornea of the WT (a, b) and *Zip13*-KO mice group (c, d). Thickness of CL, collagen fibril diameter and CFI in the WT group was higher than those in the *Zip13*-KO group. While almost all collagen fibrils in the WT group had cross-sectional alignment (b, arrowhead), those in the *Zip13*-KO group aligned in both cross-sectional (d, arrowheads) and longitudinal pattern (d, arrows). [Bars=100 nm (b, d) and 200 nm (a, c)].

fundamental on thickening of the collagenous layer. Thus, it is convincingly that the decrease of CFI is coherent with the widening distance between collagen fibrils. Reduction of ECM synthesis might be an initiation of these alterations via the blockade of Smad signaling pathway. In *Zip13*-KO fibroblast, Smad-signaling pathway having TGF-β1 stimulation was importantly for ECM synthesis [7, 8, 10]. The blockage of Smad-signalings inhibits Col1a2 mRNA expression resulting in the decrease of type I collagen synthesis in *Zip13*-KO fibroblast [7]. Although ZIP13 also existed in osteoblasts, chondrocytes, pulpal cells, and fibroblasts [7, 8], it was unclear whether keratocyte contained ZIP13. Since fibroblast and keratocyte derive from mesenchymal cell and *ZIP13* gene is relatively highly expressed in the eye of murine species [7], ZIP13 should also exist in the normal keratocyte. Regards, decrease of collagen synthesis in keratocyte in the *Zip13*-KO mice should have mechanism similarly to that in the *Zip13*-KO fibroblasts. Moreover, the differences in cellular morphology and electron density of nucleus of keratocyte in various localities should reflect the level of its transcription activity. Nucleus with a higher transcription activity must unfasten their chromatin granules so that transcription bubbles appear. Transcription could enrich RNA microenviroments to form euchromatin. Thus, the finely interspersing figures of the transcribed chromatin domains and RNA enriched microenviroments were maintained by the RNA accumulation in nucleus [9]. Such appearance finally destines the nucleus to have low electron density. In developing cornea, the bullet-shaped keratocytic stem cells with high transcription activity originally localizing in the limbus of cornea are predestined to move to the center of cornea [7, 15]. Such movement; therefore, could explain the existence of the bullet-shaped keratocytes both at the limbus and center of the cornea in the WT group. The bullet-shaped keratocytic stem cells at the limbus of cornea in *Zip13*-KO mice also travelled toward the center of cornea. During the relocation, cellular elongation also occurred together with the diminish of its transcription activity [1, 11]. Hence, transcription activity of the bullet-shaped keratocyte with low electron dense nucleus must be higher than that of the elongated keratocyte with high electron dense nucleus. Since elongated keratocytes with high electron dense nuclei were the predominant population of the central cornea of the *Zip13*-KO mice, this area surely had low transcription activity for collagen synthesis. Such reduction then became a negative impact toward the integrity of proper substance of the cornea.

The assembly of collagen fibrils to establish certain fibril diameter in cornea and elsewhere is chiefly regulated by various proteoglycans (PG) and glycosaminoglycans (GAG) [12, 18]. It has been known that dermatan sulfate increases collagen fibril diameter, but keratan sulfate inhibits the increase of collagen fibril diameter in the cornea [17]. In the *Zip13*-KO mice, the imbalance of these substances would certainly affect the fibril diameter. It is the fact that PG consists of core protein and GAG chains. Since the major PG in cornea is lumican and the GAG chain of lumican is keratan sulfate [5, 18], the loss of balance of PG components–e.g., increase of lumican or decrease of other PG (such as decorin which has dermatan sulfate as GAG chain) [18],

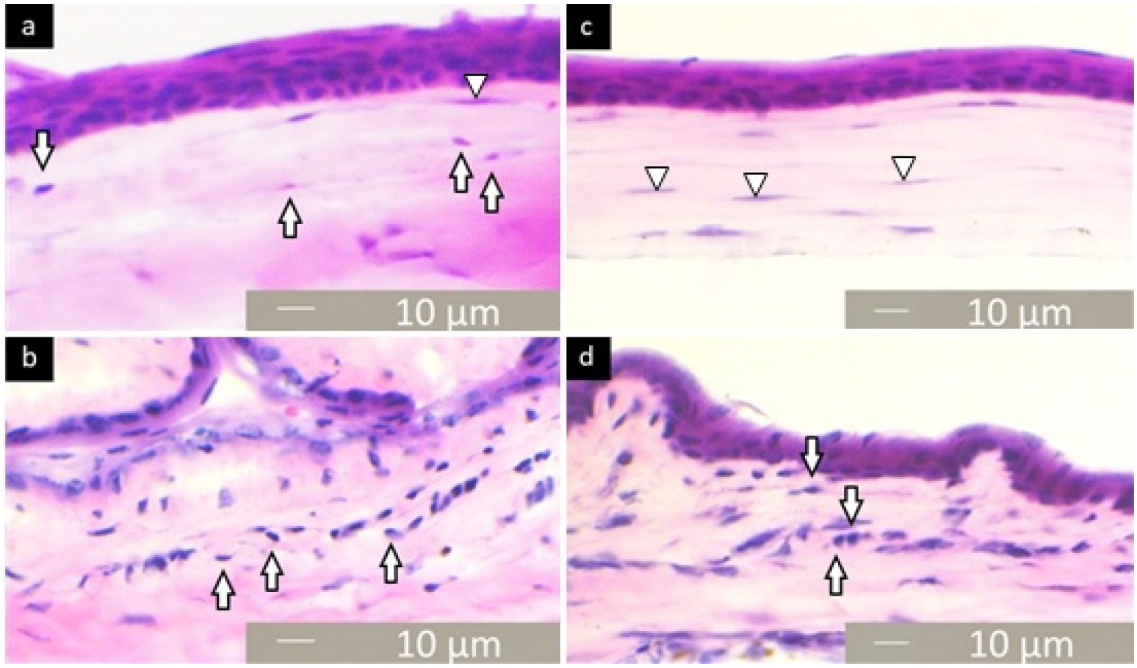

Fig. 3. Light microscopic observation of keratocytes in the center (a, c) and limbus of cornea (b, d) of the WT (a, b) and *Zip13*-KO mice group (c, d) with H&E staining. Keratocytes in the collagenous layer of the central cornea of the WT group appeared in both elongated (a, arrowhead) and bullet shape (a, arrows), while that of the *Zip13*-KO group was mainly in elongated shape (c, arrowheads). However, bullet-shaped keratocytes were the major population in the limbus of both groups (b and d, arrows). [Bars=10 μm].

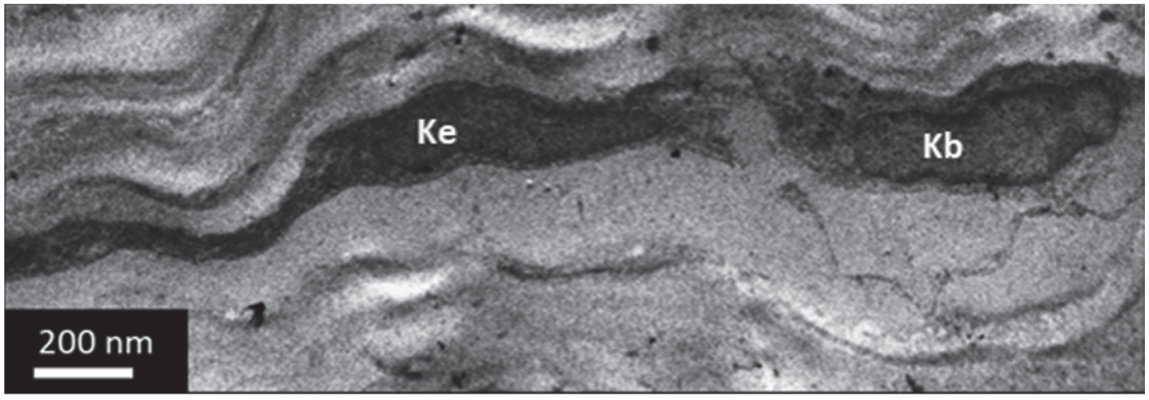

Fig. 4. TEM observation of keratocytes in the central cornea of the WT mouse. Electron density in nucleus of the elongated keratocyte (Ke) was comparatively higher than that in the bullet-shaped keratocyte (Kb). [Bar=200 nm].

would certainly affect the abnormal fibril assembly and decrease diameter of collagen fibrils. At present, the relationship between ZIP13 and GAG synthesis is still unclear. Such abnormality would decrease CFI and alter thickness and orientation of collagen fibrils. Because the transparency of cornea is regulated by a regular arranging pattern of collagen fibrils, the high degree of fibrillar misalignment would be the cause of opacity of cornea [5]. However, opaque cornea was not observed in the *Zip13*-KO mice group. It is possible that corneal opacity occurs only in the progressive spEDS cases [13].

This morphologic analysis could reveal the vulnerable characteristics of corneal stroma in the *Zip13*-KO mice. The understanding in pathologic mechanisms of various abnormalities would contribute necessary information for future research towards the alleviation of spEDS.

ACKNOWLEDGMENTS. The authors would also like to express sincere gratitude to Drs. Hiromi Ueda and Jun Minaguchi for their technical advices.

REFERENCES

1. Anthony, J. B. and Ramesh, C. T. 1997. The cornea and sclera. pp. 233–278. *In*: Wolff's Anatomy of the Eye and Orbit, 8th ed., Chapman & Hall, London.
2. Bin, B. H., Fukada, T., Hosaka, T., Yamasaki, S., Ohashi, W., Hojyo, S., Miyai, T., Nishida, K., Yokoyama, S. and Hirano, T. 2011. Biochemical characterization of human ZIP13 protein: a homo-dimerized zinc transporter involved in the spondylocheiro dysplastic Ehlers-Danlos syndrome. *J. Biol. Chem.* **286**: 40255–40265. [Medline] [CrossRef]
3. Bin, B. H., Hojyo, S., Hosaka, T., Bhin, J., Kano, H., Miyai, T., Ikeda, M., Kimura-Someya, T., Shirouzu, M., Cho, E. G., Fukue, K., Kambe, T., Ohashi, W., Kim, K. H., Seo, J., Choi, D. H., Nam, Y. J., Hwang, D., Fukunaka, A., Fujitani, Y., Yokoyama, S., Superti-Furga, A., Ikegawa, S., Lee, T. R. and Fukada, T. 2014. Molecular pathogenesis of spondylocheirodysplastic Ehlers-Danlos syndrome caused by mutant ZIP13 proteins. *EMBO Mol. Med.* **6**: 1028–1042. [Medline] [CrossRef]
4. Castori, M. and Voermans, N. C. 2014. Neurological manifestations of Ehlers-Danlos syndrome(s): A review. *Iran. J. Neurol.* **13**: 190–208. [Medline]
5. Chakravarti, S., Magnuson, T., Lass, J. H., Jepsen, K. J., LaMantia, C. and Carroll, H. 1998. Lumican regulates collagen fibril assembly: skin fragility and corneal opacity in the absence of lumican. *J. Cell Biol.* **141**: 1277–1286. [Medline] [CrossRef]
6. Deren-Wagemann, I., Kuliszkiewicz-Janus, M. and Schiller, J. 2010. The ehlers-danlos syndrome. *Adv. Exp. Med. Biol.* **19**: 537–542.
7. Fukada, T., Civic, N., Furuichi, T., Shimoda, S., Mishima, K., Higashiyama, H., Idaira, Y., Asada, Y., Kitamura, H., Yamasaki, S., Hojyo, S., Nakayama, M., Ohara, O., Koseki, H., Dos Santos, H. G., Bonafe, L., Ha-Vinh, R., Zankl, A., Unger, S., Kraenzlin, M. E., Beckmann, J. S., Saito, I., Rivolta, C., Ikegawa, S., Superti-Furga, A. and Hirano, T. 2008. The zinc transporter SLC39A13/ZIP13 is required for connective tissue development; its involvement in BMP/TGF-β signaling pathways. *PLoS ONE* **3**: e3642. [Medline] [CrossRef]
8. Hara, T., Takeda, T. A., Takagishi, T., Fukue, K., Kambe, T. and Fukada, T. 2017. Physiological roles of zinc transporters: molecular and genetic importance in zinc homeostasis. *J. Physiol. Sci.* **67**: 283–301. [Medline] [CrossRef]
9. Hilbert, L., Sata, Y., Kimura, H., Julicher, F., Honigmann, A., Zaburdaev, V. and Vastenhouw, N. 2017. Transcription establishes microenvironments that organize euchromatin. *bioRxiv*: doi: 10.1101/234112.
10. Hirose, T., Ogura, T., Tanaka, K., Minaguchi, J., Yamauchi, T., Fukada, T., Koyama, Y. and Takehana, K. 2015. Comparative study of dermal components and plasma TGF-β1 levels in Slc39a13/*Zip13*-KO mice. *J. Vet. Med. Sci.* **77**: 1385–1389. [Medline] [CrossRef]
11. Hogan, M. J., Alvarado, J. A. and Weddell, J. E. 1971. Histology of the Human Eye. Saunders, Philadelphia.
12. Iwasaki, S., Hosaka, Y., Iwasaki, T., Yamamoto, K., Nagayasu, A., Ueda, H., Kokai, Y. and Takehana, K. 2008. The modulation of collagen fibril assembly and its structure by decorin: an electron microscopic study. *Arch. Histol. Cytol.* **71**: 37–44. [Medline] [CrossRef]
13. Malfait, F., Francomano, C., Byers, P., Belmont, J., Berglund, B., Black, J., Bloom, L., Bowen, J. M., Brady, A. F., Burrows, N. P., Castori, M., Cohen, H., Colombi, M., Demirdas, S., De Backer, J., De Paepe, A., Fournel-Gigleux, S., Frank, M., Ghali, N., Giunta, C., Grahame, R., Hakim, A., Jeunemaitre, X., Johnson, D., Juul-Kristensen, B., Kapferer-Seebacher, I., Kazkaz, H., Kosho, T., Lavallee, M. E., Levy, H., Mendoza-Londono, R., Pepin, M., Pope, F. M., Reinstein, E., Robert, L., Rohrbach, M., Sanders, L., Sobey, G. J., Van Damme, T., Vandersteen, A., van Mourik, C., Voermans, N., Wheeldon, N., Zschocke, J. and Tinkle, B. 2017. The 2017 international classification of the Ehlers-Danlos syndromes. *Am. J. Med. Genet. C. Semin. Med. Genet.* **175**: 8–26. [Medline] [CrossRef]
14. Malfait, F. and De Paepe, A. 2014. The Ehlers-Danlos syndrome. *Adv. Exp. Med. Biol.* **802**: 129–143. [Medline] [CrossRef]
15. Marshall, G. E., Konstas, A. G. and Lee, W. R. 1993. Collagens in ocular tissues. *Br. J. Ophthalmol.* **77**: 515–524. [Medline] [CrossRef]
16. Munemasa, T., Idaira, Y., Fukada, T., Shimoda, S. and Asada, Y. 2014. Histological analysis of dentinogesis imperfecta in Slc39a13/ Zip13 knockout mice. *J. Hard Tissue Biol.* **23**: 163–168. [CrossRef]
17. Parry, D. A., Flint, M. H., Gillard, G. C. and Craig, A. S. 1982. A role for glycosaminoglycans in the development of collagen fibrils. *FEBS Lett.* **149**: 1–7. [Medline] [CrossRef]
18. Scott, J. E. 1992. Morphometry of cupromeronic blue-stained proteoglycan molecules in animal corneas, versus that of purified proteoglycans stained in vitro, implies that tertiary structures contribute to corneal ultrastructure. *J. Anat.* **180**: 155–164. [Medline]